Journal of Applied Polymer Science

Processing Optimization of Latex-Compounded Montmorillonite/Styrene-Butadiene Rubber-Polybutadiene Rubber

Zuguo Bao,[1] Cynthia Flanigan,[2] Laura Beyer,[2] Jie Tao[1]

[1]College of Materials Science and Technology, Nanjing University of Aeronautics and Astronautics, Nanjing 210016, China
[2]Materials and Processes Department, Research and Advanced Engineering, Ford Motor Company, Dearborn, Michigan 48124
Correspondence to: J. Tao (E-mail: taojie@nuaa.edu.cn)

ABSTRACT: Organo-montmorillonite was incorporated into model tire tread formulations through latex compounding methods, to evaluate its effects on elastomer reinforcement and dynamic properties. An intercalation structure was obtained by applying latex compounding method to prepare organoclay-emulsion stryene butadiene (E-SBR) masterbatches, for compounding with organoclay loading levels of 0–20 parts per hundred rubber (phr). Microstructure, curing properties and tire performance of the compounded rubber were investigated with the aid of X-ray diffraction, rheometor and dynamic-mechanical analysis, respectively. The results showed that organo-montmorillonite filler provided effective reinforcement in the elastomer matrix, as indicated through mechanical and dynamic mechanical properties. Tread compounds using higher organoclay loadings displayed preferred ice traction, wet traction, and dry handling, but decreased winter traction and rolling resistance. Model compounds using 15 phr of organoclay loading levels were preferred for balanced physical and dynamic properties. © 2014 Wiley Periodicals, Inc. J. Appl. Polym. Sci. **2015**, *132*, 41521.

KEYWORDS: clay; composites; mechanical properties; processing; rubber; synthesis

Received 17 February 2014; accepted 14 September 2014
DOI: 10.1002/app.41521

INTRODUCTION

Nanofillers have attracted much attention in the field of polymer technology in recent year.[1–7] Nano-reinforced elastomers have shown improved mechanical properties,[4] thermal stability,[5] wear resistance,[6] and gas permeability.[7] Layered silicates comprised of silicate layers with 1 nm thickness and up to 500 nm length are primarily selected as nanofillers in elastomers owing to their high aspect ratio.[8] Among them, montmorillonite clays have been identified as promising fillers for polymers and elastomers. The platelets can be intercalated or exfoliated by polymer chains, thus providing a large specific surface area to reinforce the matrix at low filler contents. Such intercalation or exfoliation structure was observed in Shan's detailed investigation regarding the potential applications of NR/SBR/organoclay in tire industry.[9] Mechanical reinforcement and thermal stability of the prepared nanocomposites were markedly improved with low clay content less than 5 phr. For potential applications in tire tread compounds, low filler content and enhanced filler dispersion are generally preferred for reducing hysteretic losses during elastomer deformation.[10] If used in tires, for example, this may provide a mechanism to reduce tire rolling resistance, which is a key contributor to fuel efficiency.[11]

It is difficult to achieve well-dispersed montmorillonite clay of intercalation or exfoliation structure in an elastomer matrix through traditional rubber processing method.[8] Latex compounding has been proved to be an effective method to address this problem.[12,13] Siengchin et al.[14,15] demonstrated that the latex pre-compounding master-batch method could facilitate the preparation of polystyrene-fluorohectorite nanocomposites, whereas the traditional melt compounding could not result in a nanocomposite. Actually, many types of nanoclays, including modified and pristine ones and rubber blends can also be well used for latex compounding method to obtain well-dispersed nanocomposites. [16–21] However, the existing latex compounding method needs much longer time than traditional methods to prepare nanoclay/rubber composites.[18,22,23] Therefore, it still requires additional techniques to promote mixing efficiency and further enhance intercalation and exfoliation of clay.[24,25] Potts used an ultrasonically assisted latex co-coagulation procedure to mix the thermally exfoliated graphite oxide (TEGO) with natural rubber (NR) and found that the ultrasonic treatment could promote breakup of large particles and improve the dispersion of few-layer TEGO platelets in the NR matrix.[26] This promising ultrasonic treatment was also adopted in this study as an assistant technique for latex compounding method. In addition, the effect of montmorillonite filler on the tire performances such as traction and rolling resistance is also essential to be comprehensively studied to explore the applications of montmorillonite/styrene-butadiene rubber–polybutadiene rubber (SBR-BR) in

Table I. Recipe Formulation (Parts per Hundred Rubber, By Weight)

Component	Content (phr)
Emulsion SBR (latex 69.8%)	37.5
Solution SBR (oil extended)[a]	51.56
Polybutadiene rubber	25
N234 carbon black	30
Nano-clay, Cloisite 20A	0~20[b]
Processing oil, RAE	10
Zinc oxide	1.9
Microcrystalline wax	2
Antiozonant[c]	2
Antioxidant[d]	0.5
Stearic acid	1.5
Processing aid	2
Sulfur	1.5
TBBS[e]	1.3
DPG[f]	1.5
Total phr	168.26-188.26

[a] Oil content is 27.3% by weight.
[b] The recipe name of MX denotes clay loadings of X parts per hundred rubber (phr) in the rubber compound.
[c] (*N*-(1,3-dimethyl butyl) *N*′-phenyl-*p*-phenylene diamine).
[d] 2,2,4-trimethyl-1,2-dihydroquinoline.
[e] Tert-butyl-2-benzothiazyl sulfonamide.
[f] Diphenyl guanidine.

tire industry. In this study, organo-montmorillonite was introduced in rubber using a two-tiered approach: optimization of processing parameters and incorporation into a model tread formulation. Latex compounding was used to improve the dispersion of the clay in the rubber matrix and to evaluate preferred processing methods for rubber reinforcement. Ultrasonication and addition of ethanol were used to amend traditional latex compounding methods to obtain a more effective and better filler dispersion. Then, the processing parameters, curing properties, physical properties, and tire performance predictors were investigated for various loading levels. Finally, optimized latex compounding parameters and filler loading levels were determined based on experiment results.

EXPERIMENTAL

Materials

Carbon black (N234, Cabot Corporation) and natural montmorillonite modified with a quaternary ammonium salt ($d_{001} = 24.2$Å, Cloisite 20A, Southern Clay Products) were used as reinforcing fillers in a mould rubber. During the latex compounding, emulsion styrene-butadiene rubber (E-SBR) latex [Bound styrene content = 23.75%, Mooney viscosity ML(1+4)100°C = 130, 69.8% of solid content, LPF5356, Goodyear] was used to disperse the organoclay in rubber. The elastomers used in this study also included Buna VSL 5025-2, a solution-SBR with 50% vinyl and 25% styrene content [Mooney viscosity ML(1+4)100°C = 62, $T_g = -29$°C], and Buna CB 1203, a solution high cis [Mooney viscosity ML(1+4)100°C = 62, cis-1,4 content 96%] polybutadiene, both supplied by Lanxess. Table I provides an overview of key chemical ingredients used in the experiments.

Processing

The organo-montmorillonite filler and E-SBR were mixed by a latex compounding method. The organoclay was first suspended in a solution of ethanol and deionized water (0/100 to 50/50 by weight). The mixture was then ultrasonicated and stirred for a given period of time. The latex was added into the slurry and stirred for another 30 min. Finally, the mixture was cast into a shallow container and dried in an oven at 50°C.

The formation process of organoclay–rubber intercalation during latex compounding is depicted in Figure 1. The mixing process needs to supply sufficient surface contact and time for the intercalation reaction. Varying levels of ethanol, water, and ultrasonication times were used to achieve this goal. At first, the organoclay was dispersed in water and ethanol mixing solution [Figure. 1(a)]. Ethanol was introduced to improve the wettability of water on organoclay surface, avoiding the formation of large organoclay conglomerations on the solution surface. Ultrasonication and stirring were then applied to break up the organoclay agglomeration and form well-dispersed particles in the mixture [Figure. 1(b)]. The usages of ethanol and ultrasonication processing were new amendments that brought favorable filler dispersion but reduced the time and energy when compared with previous studies. Finally, the latex was added in the slurry, and the intercalated organoclay was obtained after stirring for another 30 min [Figure. 1(c)].

The rubber and fillers were compounded in a Farrell Model 2.6 BR Banbury Mixer with a 70% fill factor. A three-stage mixing process was used, in which the elastomers, fillers, and processing oil were added in the first pass. The sulfur and accelerator ingredients were mixed with the master batch in the final pass. The mixing time and temperature for three processing steps were 4 min at 160°C, 5.5 min at 160°C, and 3min at 110°C, respectively. After each pass, the compound was sheeted out on a two-roll mill. Following the productive pass, the compound was compressively moulded as described in reference.[10]

Characterization and Measurements

Physical properties of the cured samples were evaluated for tensile strength, modulus, elongation, tear resistance, and hardness. Tensile properties were tested according to ASTM D 412, Test Method A, Die C.[27] Shore A hardness was measured as directed in ASTM D 2240.[28] Tear strength was assessed according to ASTM D 624.[29]

Intercalation structure of the composite was measured by X-ray diffraction (XRD), which was performed on a Scintag X-ray diffractometer with Cu Kα radiation ($\lambda = 1.541$ Å, 45 kV, 40 mA) in the 2θ range of 1.5°–30°. A thin film pasted on a zero-diffraction glass was used to characterize the structure of latex compounded master batch.

Dynamic-mechanical analysis (DMA) was conducted on rectangular specimens in tensile mode at a frequency of 1 Hz using a DMA/SDTA861e system from Mettler Toledo, Switzerland. Storage modulus (E'), loss modulus (E''), complex modulus (E^*), and loss factor (tangent $\delta = E''/E'$) were obtained through temperature sweeps in the range −40 to 70°C at a heating rate of 1°C/min. The

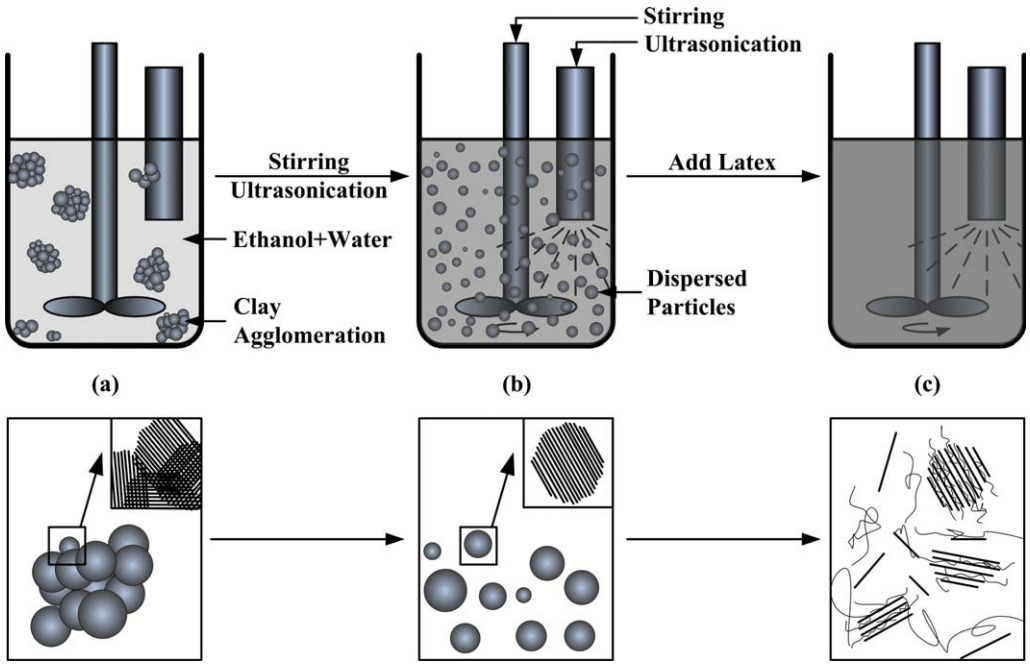

Figure 1. Formation of the intercalation structure during latex compounding. [Color figure can be viewed in the online issue, which is available at wileyonlinelibrary.com.]

maximum amplitude and displacement were set as 10 N and 25 μm, respectively. Modulus in small strain region (<3%) was obtained through strain sweep testing at 30°C and 1 Hz.

RESULTS AND DISCUSSIONS

Optimization of Latex Compounding Parameters

Organo-montmorillonite could be intercalated by rubber molecules through latex compounding, as shown in Figure 2. The processing parameters are listed in Table II. The organoclay exhibits a diffraction peak corresponding to 2.6 nm, which is close to the reported value ($d_{001} = 2.4$ nm). For the optimized processing parameters of latex compounding, the organoclay is intercalated by rubber molecules with a d-space of 4.2 nm.

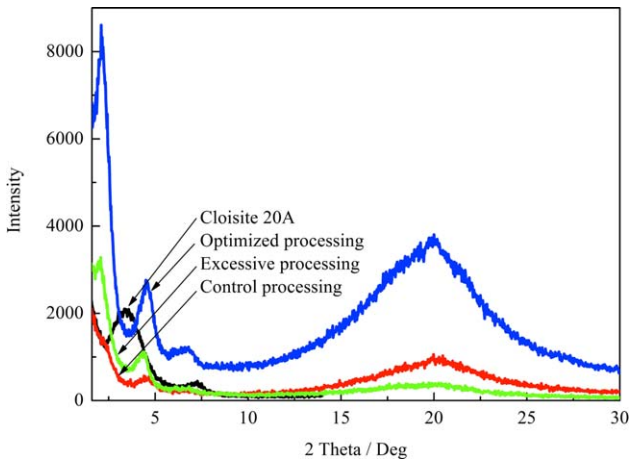

Figure 2. XRD patterns of organoclay and its master batch using three processing methods. [Color figure can be viewed in the online issue, which is available at wileyonlinelibrary.com.]

Increased levels of water and ethanol, or longer ultrasonication time (excessive processing) do not improve the intercalation ($d = 4.2$ nm). However, the organoclay forms only agglomerations (no intercalation) if none of these processing aids are used in latex compounding, shown by the control sample of $d = 2.0$ nm. The reason for this confinement is unclear so far. The diffraction peaks at $2\theta = 20°$ belong to the SBR,[30] and their incomparable diffraction intensities probably result from the thickness differences among the film samples. The d-space of organoclay is expanded by 1.6 nm through optimized latex compounding process. Based on the XRD results, optimized processing parameters for latex compounding are 20% of organoclay/ethanol solution, 10% organoclay/water solution, and 120 min for ultrasonication.

The morphology and structure of the organo-montmorillonite–filled rubber through optimized latex compounding are displayed in Figure 3. The dark shadows observed in Figure 3(a) are the agglomerated carbon black particles. The montmorillonite possesses a good dispersion in the rubber matrix. Most of montmorillonite organoclay exhibits flocculation microstructure instead of the aggregate particles, as shown in Figure 3(a). Intercalation structure is confirmed with a higher magnification image of Figure 3(b), showing one of the stacks of

Table II. Latex Compounding Parameters of Three Processing Methods

Processing methods	Ethanol (%)	Water (%)	Ultrasonication (min)
Control processing	0	0	0
Excessive processing	10	1	1200
Optimized processing	20	10	120

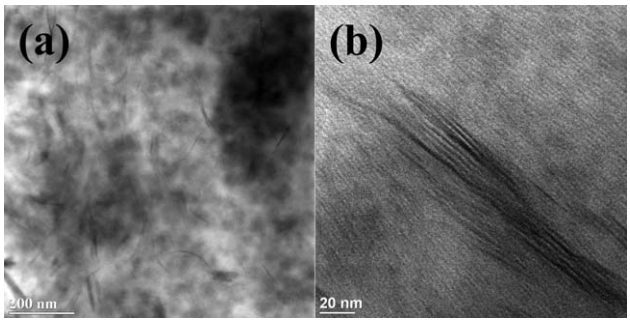

Figure 3. TEM images of organoclay filled rubber (M5).

Table III. Curing Properties of Organoclay–Rubber Master Batch with Different Latex Compounding Process

Curing properties	M5	M5 control	M20	M20 control
Max. torque (Nm)	5.49	5.62	4.16	4.23
Min. torque (Nm)	1.22	1.24	1.04	1.13
ΔTorque (Nm)	4.27	4.38	3.12	3.10
t_{s02} (min)	1.67	1.64	1.88	1.76
t_{c90} (min)	7.91	7.83	13.14	12.74
CRI (min^{-1})	16.03	16.16	8.88	9.11

montmorillonite lamellaes. The *d*-space of intercalated rubber is about 3.7 nm. This smaller *d*-space than XRD results is mainly caused by the different testing principles of two techniques.

Figure 4 displays XRD patterns of cured rubber samples containing organoclay/E-SBR master batches from different latex compounding processes. Compared with organoclay/E-SBR master batches, the interlayer *d*-space of organoclay in the cured rubber prepared by control latex compounding (M20 Control and M5 Control) is expanded from 2.0 to 4.2 nm, indicating that the subsequent melt compounding, including Banbury and two-roll mill mixing process, also helps with the organoclay intercalation. Such melting intercalation for organoclay was also confirmed by other researchers.[8] For the optimized latex compounding, the *d*-space of organoclay in cured rubber ($d = 4.3$nm) is the same as that in the master batches. The melting compounding process fails to further expand the interlayer space of the organoclay.

The curing kinetics of organoclay–rubber compounds are presented in Table III. It can be seen that the latex compounding process has a slight effect on the maximum torque, the minimum torque, and cure rate index ($CRI = 100/(t_{c90} - t_{s02})$, min^{-1}). The agglomerations remaining after the control latex compounding may not break up completely during the subsequent mixing and compression moulding steps. The absence of the diffraction peaks of these agglomerations may result from the small content and the overlapping band with diffraction peak on crystal plane (002) of intercalated organo-montmorillonite. Therefore, the agglomeration in the control-processed samples decreases the average distance between sulfur and rubber molecules, which promotes the curing reaction and causes decreased scorch time (t_{s02}) when compared with optimally processed samples. As listed in Table III, the maximum torque, the minimum torque, and cure rate index of control samples are larger than those of their counterparts.

The existence of organoclay agglomeration in the control samples is also evident when the filler network is investigated through strain sweep of cured samples. Figure 5 displays the storage modulus (E') of organoclay-filled rubber in the small strain region. With the same loadings, the higher initial modulus combined with larger change in modulus from 0 to 3% strain of the control-processed samples indicate a stronger filler–filler network in the rubber composites. It is believed that the filler–filler network in the small strain region is determined by the completeness of filler dispersion.[31] In other words, elastomer compounds using the control processing methods exhibits larger Payne Effect, indicating poorer dispersion of the fillers.[32]

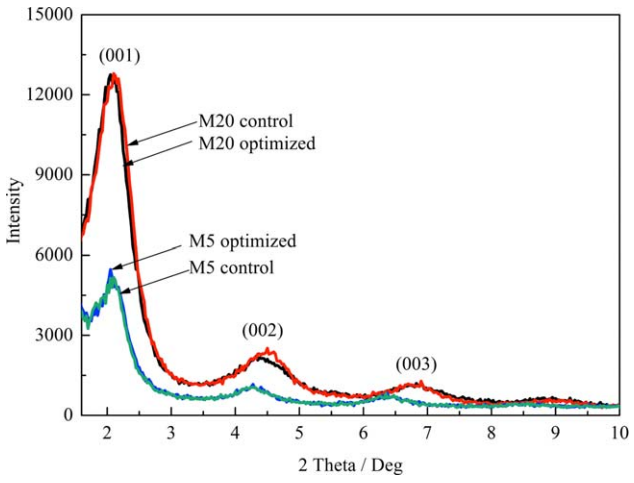

Figure 4. XRD patterns of organoclay filled rubber with different latex compounding processes. [Color figure can be viewed in the online issue, which is available at wileyonlinelibrary.com.]

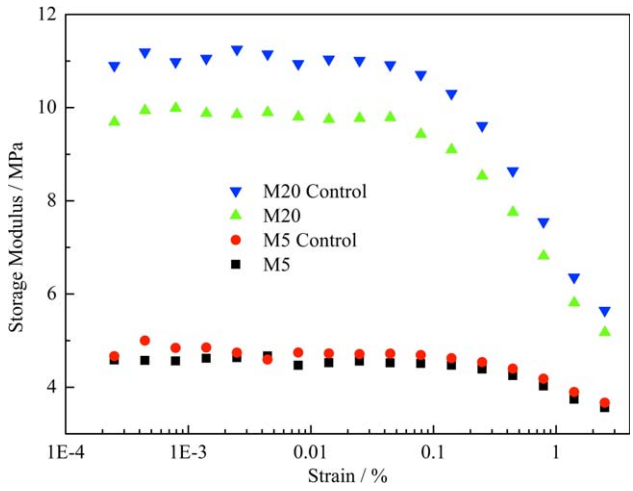

Figure 5. Strain sweep of organoclay filled rubber with different latex compounding process. [Color figure can be viewed in the online issue, which is available at wileyonlinelibrary.com.]

Table IV. Mechanical Properties of Cured Rubber with Different Latex Compounding Process

Physical Properties	M5	M5 Control	M20	M20 Control
Tensile stress (MPa)	13.8 ± 0.8	13.9 ± 0.3	16.2 ± 1.1	16.8 ± 1.4
Elongation (%)	543 ± 11	528 ± 9	638 ± 21	626 ± 22
Modulus @ 300% (MPa)	5.10 ± 0.22	5.46 ± 0.24	4.66 ± 0.17	5.13 ± 0.29
Modulus @ 100% (MPa)	1.24 ± 0.05	1.31 ± 0.07	1.33 ± 0.04	1.37 ± 0.08
Reinforcement index[a]	4.12 ± 0.03	4.17 ± 0.04	3.51 ± 0.03	3.74 ± 0.03
Tear resistance (k Nm^{-1})	21.6 ± 1.4	21.9 ± 3.2	24.2 ± 1.1	22.7 ± 0.4
Shore A hardness	52.1 ± 0.4	53.4 ± 0.4	53.6 ± 0.4	55.7 ± 0.4

[a] Reinforcement Index = $\frac{\text{Modulus@300\%}}{\text{Modulus@100\%}}$.

The mechanical properties of the cured rubber are listed in Table IV. The impact of latex compounding process on the modulus is consistent with the strain sweep data discussed above. The slight reduction in elongation and tear resistance of the control processed samples may be caused by the agglomeration of organoclay. Because Banbury mixing and compression moulding likely break up most of the agglomerations formed during the latex compounding, the samples prepared through optimized and control processing methods possess close mechanical properties.

To obtain good performances of organo-montmorillonite–filled rubber as tire treads, several parameters, including high (wet, ice, and winter) traction, high wear resistance, low rolling resistance, and high dry handling, are required by the researchers. These key performances of tire treads depends largely on the viscoelastic behavior of filler-filled rubber.[33,34] Many researchers have investigated the correlations between certain viscoelastic properties and tire performances.[35,36] For example, a lower loss factor (tangent δ) at low frequency leads to lower rolling resistance.[37,38] Thus, DMA is often used to predict the performance of tread compounds under different environmental conditions. As shown in Table V, the traction, handling, and rolling resistance was predicted by comparing the values of storage modulus (E') and loss factor (tangent δ) at certain temperatures. Other than dry handling, most of the tread displayed close values, indicating negligible influence of latex compounding on the predicted tire performance.

Table V. Tire Performance Predicted by DMA (Comparing Latex Compounding Processes)

Predicted performance	M5	M5 control	M20	M20 control
Winter traction E' @ −20°C (MPa) (lower is better)	31.21	31.96	74.78	72.94
Ice traction Tan δ @ −10°C (higher is better)	0.366	0.363	0.403	0.370
Wet traction Tan δ @ 10°C (higher is better)	0.181	0.179	0.222	0.219
Dry handling E' @ 30°C (MPa) (higher is better)	4.26	4.45	7.28	7.96
Rolling resistance Tan δ @ 60°C (lower is better)	0.079	0.076	0.128	0.127

Effect of Organoclay Loading on Properties of Rubber Composites

The XRD patterns of cured rubber with loadings of 0–20 phr are shown in Figure 6, which demonstrates that intercalation structures of the nanoclay–rubber are not affected by varying organoclay loading levels. The increasing filler loadings bring about the increasing intensities of the diffraction peaks, but without having an effect on the diffraction angles.

The effect of increasing nanoclay loading levels on elastomeric curing kinetics is presented in Table VI. With higher loading of nanoclay filler, both the extent of curing (indicated by ΔTorque values) and cure rate index (CRI, rate of vulcanization) decreases. The similar influences of nanoclay on the curing properties were also reported by other researchers.[22] The addition of organoclay filler occupies volume in the rubber matrix, affecting the ability of polymer chains to cross-link. In addition, incorporation of nanoclay filler decreases the crosslink density in the elastomer matrix, providing a lower torque and extent of

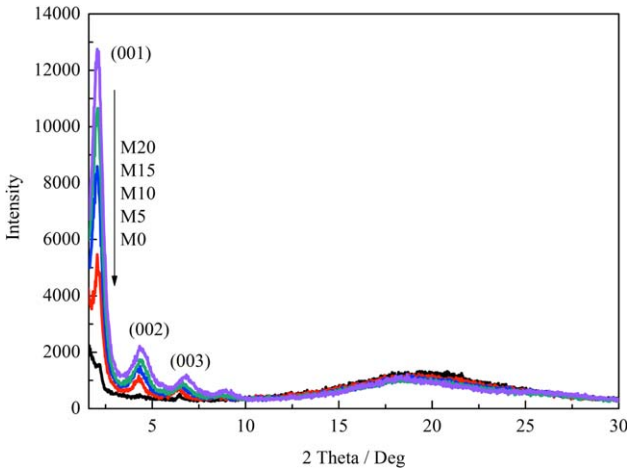

Figure 6. XRD patterns of cured rubber with different organoclay loadings. [Color figure can be viewed in the online issue, which is available at wileyonlinelibrary.com.]

Table VI. Curing Properties of Organoclay–Rubber Compound with Different Organoclay Loadings

Curing properties	M0	M5	M10	M15	M20
Max. torque (Nm)	5.32	5.49	5.18	4.61	4.16
Min. torque (Nm)	1.14	1.22	1.12	1.10	1.04
ΔTorque (Nm)	4.18	4.27	4.06	3.51	3.12
t_{s02} (min)	2.34	1.67	1.71	1.79	1.88
t_{c90} (min)	7.62	7.91	10.00	10.87	13.14
CRI (min^{-1})	18.94	16.03	12.06	11.01	8.88

curing reaction. Another effect is the increase in distance between sulfur and rubber molecules, which causes prolonged curing times (t_{c90}) and depressed curing rates. These influences become more severe when the loading of the organo-montmorillonite is increased. With loading of 20 phr organo-clay, the extent of curing and cure rate index are decreased by 25 and 53%, respectively, when compared with rubber compounds without additional organoclay filler.

The filler network was investigated through analyzing strain sweeps of cured samples with varied organoclay loading levels, as seen in Figure 7. Samples with increased levels of organoclay filler exhibits higher initial modulus and Payne Effect.[32] Higher initial modulus resulted from stronger filler–filler interaction owing to the shorter distance among reinforcing filler aggregates in the higher-loading samples. The modulus declines as the strain raises, implying that such filler–filler interactions are weak and can break down even under small strain (<1%) deformation. The Van der Waals forces among organoclay fillers fall off markedly with the increasing distance among fillers.[25] It is believed that the energy dissipated from the breakdown and reconstruction of filler–filler network during cyclical deformation is the main source of rolling resistance of automotive tires. Therefore, lower Payne Effect at smaller organoclay loadings is favorable for fuel economy considerations of tires.

The mechanical properties of the cured rubber with organoclay loading varying from 0 to 20 phr are listed in Table VII. Key physical properties, including tensile strength, percent elongation to break, tear resistance, and Shore A hardness, are improved as the amount of organoclay reinforcement increased. This trend confirmed that the organoclay filler aids in reinforcing the elastomer matrix. Similar results were also obtained for the changes of various clay/rubber nanocomposites.[39–42] The strength and elongation increased for good organoclay dispersion and relatively low organoclay content. Although high organoclay content produced saturation and deterioration in strength and elongation of the nanocomposites, this may be related with the premature failure caused by the agglomerations at high filler loadings.[39] The modulus change is consistent with the strain sweep results. Samples with 15 phr organoclay loading levels exhibited preferred mechanical properties. Higher loading (20 phr) rubber composite displayed similar or lower physical properties to the 15-phr compounds. This result is attributed to the increasing probability of agglomeration when approaching the saturation volume of reinforcing filler content.

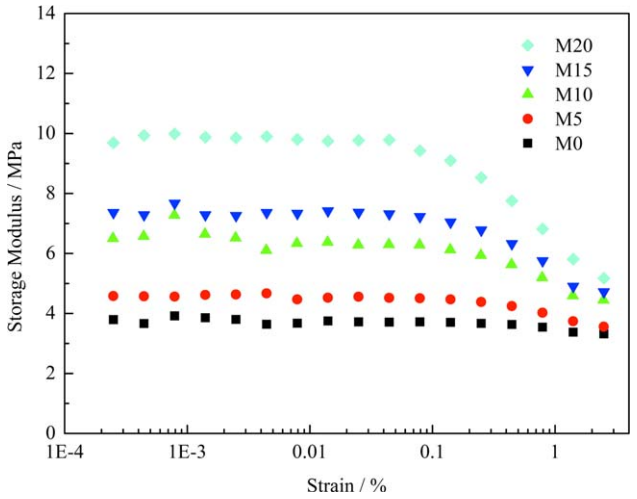

Figure 7. Strain sweep of organoclay filled rubber with different filler loading. [Color figure can be viewed in the online issue, which is available at wileyonlinelibrary.com.]

The performances of tread compounds with different organo-montmorillonite loadings are listed in Table VIII. Tread compounds with higher organoclay loadings display better ice traction, wet traction, and dry handling, but worse winter traction and rolling resistance. Tangent delta values at 60°C (predictor for rolling resistance) are influenced by the total volume fraction of the filler.[11] With an increase in organoclay loading levels, tangent δ values increase significantly. Therefore, the organoclay loading should be determined by considering these trade-offs

Table VII. Mechanical Properties of Cured Rubber with Different Organoclay Loadings

Physical properties	M0	M5	M10	M15	M20
Tensile stress (MPa)	10.4 ± 0.9	13.8 ± 0.8	14.6 ± 0.7	16.2 ± 1.2	16.2 ± 1.1
Elongation (%)	461 ± 8	543 ± 11	567 ± 21	620 ± 33	638 ± 21
Modulus @ 300% (MPa)	5.05 ± 0.34	5.10 ± 0.22	5.30 ± 0.32	5.05 ± 0.32	4.66 ± 0.17
Modulus @ 100% (MPa)	1.23 ± 0.06	1.24 ± 0.05	1.32 ± 0.11	1.32 ± 0.11	1.33 ± 0.04
Reinforcement index	4.10 ± 0.07	4.12 ± 0.03	4.02 ± 0.10	3.83 ± 0.07	3.51 ± 0.03
Tear resistance (k Nm^{-1})	23.2 ± 2.0	21.6 ± 1.4	23.5 ± 1.6	25.3 ± 2.8	24.2 ± 1.1
Shore A hardness	51.8 ± 0.29	52.1 ± 0.40	54.0 ± 0.34	54.2 ± 0.37	53.6 ± 0.36

Table VIII. Tire Performance Predicted by DMA (Different Organoclay Loadings)

Predicted performance	M0	M5	M10	M15	M20
Winter traction E' @ −20°C (MPa) (lower is better)	23.41	31.21	43.29	63.24	74.78
Ice traction Tan δ @ −10°C (higher is better)	0.385	0.366	0.375	0.412	0.403
Wet traction Tan δ @ 10°C (higher is better)	0.177	0.181	0.207	0.215	0.222
Dry handling E' @ 30°C (MPa) (higher is better)	3.67	4.26	4.76	6.19	7.28
Rolling resistance Tan δ @ 60°C (lower is better)	0.060	0.079	0.093	0.100	0.128

and mechanical properties. Within this experimental study, rubber composites containing 15 phr of montmorillonite are preferred for balanced physical and dynamic properties.

It is important to note that silica fillers are often used in tire tread recipes, especially those that focus on low rolling resistance requirement. The scope of this study was limited to carbon black and nanoclay fillers, in an effort to reduce complexity of the variables. Owing to their similar inorganic nature, the interaction between silica and layered silicates needs to be investigated in the future when they are used simultaneously as fillers in tread formulation designs.

In addition, this study evaluated the effect of organomontmorillonite loading levels on model elastomer compounds, including tire performance predictors such as traction and rolling resistance. In practice, wear resistance also needs to be assessed during tread rubber formulation development. Empirically, wear resistance is optimal when the volume fraction of reinforcing fillers is about 20–25%.[11] For the optimized organoclay loading of 15 phr (containing 30 phr of carbon black), the calculated volume fraction is around 15%. There are many future opportunities to optimize trade-offs among the three key performances of traction, wear, and rolling resistance.

CONCLUSIONS

Organoclay fillers were introduced into formulations of model tread compounds through latex compounding methods. Intercalated structure was obtained in the latex-compounded master batch by optimizing processing parameters, including premixing of 20% organoclay/ethanol solutions, 10% organoclay/water solutions, and 120 min of ultrasonication. The nanoclay intercalation structure was not affected by the addition of organoclay loading levels up to 20 phr. The increase in nanoclay filler in the elastomer matrix affected curing properties, as indicated by the decrease in maximum torque, minimum torque, extent of cure, and cure rate index. Filler–filler interactions with high loading levels of organoclay were concluded through dynamic strain sweep tests. Use of organoclays provided a reinforcing effect on mechanical properties in the rubber compounds. For the nanoclay-filled model elastomer compounds, dynamic mechanical analysis performance predictors were used to assess potential reinforcement for tire tread applications by comparing loss factors at various temperatures. Compounds with higher organoclay loadings displayed improved ice traction, wet traction, and dry handling. Increased loading levels of nanoclays did not improve performance predictors for winter traction or rolling resistance. Within this experimental study, rubber composites containing 15 phr of montmorillonite were preferred for balanced physical and dynamic properties.

ACKNOWLEDGMENTS

This work was supported by Ford China University Research Program (No. 2009–5041R), Funding of Jiangsu Innovation Program for Graduate Education (No. CXLX11_0189) and Nanjing University of Aeronautics and Astronautics Research Funding (No.1006-KFA13731). The authors thank Lanxess Corporation, Cabot Corporation, Akrochem Corporation, HollyFrontier, Goodyear Chemical, and Southern Clay Products for the donation of chemicals used in this study. In addition, Sarah Hetzler is thanked for her previous work and Andy Drews for his technical input for X-ray diffraction analysis.

REFERENCES

1. Maiti, M.; Bhattacharya, M.; Bhowmick, A. *Rubber Chem. Technol.* **2008**, *81*, 384.
2. Ke, Y. C.; Stroeve, P. Polymer-Layered Silicate and Silica Nanocomposites; Elsevier: Amsterdam, **2005**; Chapter *1*, p 3.
3. Pavlidou, S.; Papaspyrides, C. *Prog. Polym. Sci.* **2008**, *33*, 1119.
4. Valadares, L.; Leite, C.; Galembeck, F. *Polymer* **2006**, *47*, 672.
5. Mohan, T.; Kuriakose, J.; Kanny, K. *J. Ind. Eng. Chem.* **2011**, *17*, 264.
6. Tabsan, N.; Wirasate, S.; Suchiva, K. *Wear* **2010**, *269*, 394.
7. Liang, Y.; Cao, W.; Li, Z. *Polym. Test.* **2008**, *27*, 270.
8. Varghese, S.; Karger-Kocsis, J. *Polymer* **2003**, *44*, 4921.
9. Shan, C.; Gu, Z.; Wang, L.; Li, P.; Song, G.; Gao, Z.; Yang, X. *J. Appl. Polym. Sci.* **2011**, *119*, 1185.
10. Flanigan, C.; Beyer, L.; Klekamp, D.; Rohweder, D.; Stuck, B.; Terrill, E. *Rubber World* **2012**, *245*, 18.
11. U.S. Department of Transportation. The Pneumatic Tire; National Highway Traffic Safety Administration, **2006**; Chapter *12*, p 504.
12. Rezende, C.; Braganca, F.; Doi, T.; Lee, L.; Galembeck, F.; Boue, F. *Polymer* **2010**, *51*, 3644.
13. Chakraborty, S.; Kar, S.; Dasgupta, S.; Mukhopadhyay, R.; Bandyopadhyay, S.; Joshi, M.; Ameta, S. *Polym. Test.* **2010**, *29*, 181.
14. Siengchin, S.; Karger-Kocsis, J.; Apostolov, A.; Thomann, R. *J. Appl. Polym. Sci.* **2007**, *106*, 248.

15. Siengchin, S.; Karger-Kocsis, J. *Macromol. Rapid Commun.* **2006**, *27*, 2090.
16. Wu, Y.; Wang, Y.; Zhang, H.; Wang, Y.; Yu, D.; Zhang, L.; Yang, J. *Compos. Sci. Technol.* **2005**, *65*, 1195.
17. Varghese, S.; Gatos, K.; Apostolov, A.; Karger-Kocsis, J. *J. Appl. Polym. Sci.* **2004**, *92*, 543.
18. Pojanavaraphan, T.; Magaraphan, R. *Eur. Polym. J.* **2008**, *44*, 1968.
19. Jia, Q.; Wu, Y.; Wang, Y.; Lu, M.; Zhang, L. *Compos. Sci. Technol.* **2008**, *68*, 1050.
20. Boonmahitthisud, A.; Chuayjuljit, S. *Adv. Mater. Res.* **2012**, *347*, 3197.
21. Stephen, R.; Ranganathaiah, C.; Varghese, S.; Joseph, K.; Thomas, S. *Polymer* **2006**, *47*, 858.
22. Tan, J.; Wang, X.; Luo, Y.; Jia, D. *Mater. Des.* **2012**, *34*, 825.
23. Chakraborty, S.; Sengupta, R.; Dasgupta, S.; Mukhopadhyay, R.; Bandyopadhyay, S.; Joshi, M.; Ameta, S. *J. Appl. Polym. Sci.* **2009**, *113*, 1316.
24. Bhowmick, A.; Bhattacharya, M.; Mitra, S. *J. Elastomers Plast.* **2010**, *42*, 517.
25. Jia, Q.; Wu, Y.; Wang, Y.; Lu, M.; Yang, J.; Zhang, L. *J. Appl. Polym. Sci.* **2007**, *103*, 1826.
26. Potts, J.; Shankar, O.; Murali, S.; Du, L.; Ruoff, R. *Compos. Sci. Technol.* **2013**, *74*, 166.
27. ASTM D 412 Standard Test Methods for Vulcanized Rubber and Thermoplastic Elastomers-Tension, **2002**.
28. ASTM D 2240 Standard Test Methods for Rubber Property-Durometer Hardness, **2005**.
29. ASTM D 624 Standard Test Method for Tear Strength of Conventional Vulcanized Rubber and Thermoplastic Elastomers, **2000**.
30. Malas, A.; Pal, P.; Giri, S.; Mandal, A.; Das, C. *Compos. Part B* **2014**, *58*, 267.
31. Frohlich, J.; Niedermeier, W.; Luginsland, H. *Compos. Part A* **2005**, *36*, 449.
32. Gauthiera, C.; Reynauda, E.; Vassoillea, R.; Ladouce-Stelandre, L. *Polymer* **2004**, *45*, 2761.
33. Mihara, S. Reactive Processing of Silica-Reinforced Tire Rubber; University of Twente:, **2009**; Chapter *2*, p 6.
34. U.S. Department of Transportation. Dynamic Mechanical Properties of Passenger and Light Truck Tire Treads; National Highway Traffic Safety Administration, **2010**; p 1.
35. Hall, D.; Moreland, J. *Rubber Chem. Technol.* **2001**, *74*, 525.
36. Heinrich, G. *Kautsch. Gummi Kunstst.* **1992**, *45*, 173.
37. Nordsiek, K. *Kautsch. Gummi Kunstst.* **1985**, *38*, 178.
38. Wang, M. *Rubber Chem. Technol.* **1998**, *71*, 520.
39. Gatos, K.; Karger-Kocsis, J. *Polymer* **2005**, *46*, 3069.
40. Chang, Y.; Yang, Y.; Ryu, S.; Nah, C. *Polym. Int.* **2002**, *51*, 319.
41. Kim, J.; Oh, T.; Lee, D. *Polym. Int.* **2003**, *52*, 1058.
42. Pramanic, M.; Srivastava, S.; Samantary, B.; Bhowmick, A. *J. Polym. Sci.* **2002**, *40*, 2065.